

# Journal of Visualized Experiments

## Visualization and quantification of brown and beige adipose tissues in mice using [18F]FDG micro-PET/MR imaging --Manuscript Draft--

Article Type:	Invited Methods Article - JoVE Produced Video
Manuscript Number:	JoVE62460R1
Full Title:	Visualization and quantification of brown and beige adipose tissues in mice using [18F]FDG micro-PET/MR imaging
Corresponding Author:	Xiaoyan Hui Hong Kong University: University of Hong Kong Hong kong, HONG kong HONG KONG
Corresponding Author's Institution:	Hong Kong University: University of Hong Kong
Corresponding Author E-Mail:	hannahui@hku.hk
Order of Authors:	Qing Liu Kel Vin Tan Hing-Chiu Chang Pek-Lan Kwong Xiaoyan Hui
Additional Information:	
Question	Response
Please indicate whether this article will be Standard Access or Open Access.	Standard Access (US\$2,400)
Please specify the section of the submitted manuscript.	Biology
Please indicate the <b>city, state/province, and country</b> where this article will be <b>filmed</b> . Please do not use abbreviations.	Hong Kong SAR
Please confirm that you have read and agree to the terms and conditions of the author license agreement that applies below:	I agree to the <a href="#">Author License Agreement</a>
Please provide any comments to the journal here.	
Please indicate whether this article will be Standard Access or Open Access.	Standard Access (\$1400)

**TITLE:**

Visualization and Quantification of Brown and Beige Adipose Tissues in Mice using [ $^{18}\text{F}$ ]FDG Micro-PET/MR Imaging

**AUTHORS AND AFFILIATIONS:**

Qing Liu<sup>1,2\*</sup>, Kel Vin Tan<sup>3\*</sup>, Hing-Chiu Chang<sup>3</sup>, Pek-Lan Kwong<sup>3</sup>, Xiaoyan Hui<sup>1,2,4</sup>

<sup>1</sup>State Key Laboratory of Pharmaceutical Biotechnology, The University of Hong Kong, Pokfulam, Hong Kong SAR, China

<sup>2</sup>Department of Medicine, Li Ka Shing Faculty of Medicine, The University of Hong Kong, Pokfulam, Hong Kong SAR, China

<sup>3</sup>Department of Diagnostic Radiology, Li Ka Shing Faculty of Medicine, The University of Hong Kong, Pokfulam, Hong Kong SAR, China

<sup>4</sup>School of Biomedical Sciences, Institute of Vascular Medicine, Chinese University of Hong Kong, Hong Kong, China.

\*These authors contributed equally to this manuscript.

Email addresses of co-authors:

Qing Liu	(lexielq@hku.hk)
Kel Vin Tan	(kvtan@hku.hk)
Hing-Chiu Chang	(hcchang@hku.hk)
Pek-Lan Kwong	(plkhong@hku.hk)
Xiaoyan Hui	(hannahui@hku.hk)

Corresponding author:

Xiaoyan Hui (hannahui@hku.hk)

**KEYWORDS:**

brown adipose tissue, beige adipocytes, thermogenesis, glucose uptake, micro-PET/MR imaging, [ $^{18}\text{F}$ ]FDG

**SUMMARY:**

Functional imaging and quantitation of thermogenic adipose depots in mice using a micro-PET/MR imaging-based approach.

**ABSTRACT:**

Brown and beige adipocytes are now recognized as potential therapeutic targets for obesity and metabolic syndromes. Non-invasive molecular imaging methods are essential to provide critical insights into these thermogenic adipose depots. Here, the protocol presents a PET/MR imaging-based method to evaluate the activity of brown and beige adipocytes in mouse interscapular brown adipose tissue (iBAT) and inguinal subcutaneous white adipose tissue (iWAT). Visualization and quantification of the thermogenic adipose depots were achieved using [ $^{18}\text{F}$ ]FDG, the non-metabolizable glucose analog, as the radiotracer, when combined with the precise anatomical

information provided by MR imaging. The PET/MR imaging was conducted 7 days after cold acclimation and quantitation of [ $^{18}\text{F}$ ]FDG signal in different adipose depots was conducted to assess the relative mobilization of thermogenic adipose tissues. Removal of iBAT substantially increased cold-evoked [ $^{18}\text{F}$ ]FDG uptake in iWAT of the mice.

## INTRODUCTION:

In response to changing nutritional needs, adipose tissue serves as an energy cache to adopt either lipid storage or mobilization mode to meet the needs of the body<sup>1</sup>. Moreover, adipose tissue also plays a key function in thermoregulation, via a process called non-shivering thermogenesis, also called facultative thermogenesis. This is typically achieved by the brown adipose tissue (BAT), which expresses abundant level of mitochondria membrane protein uncoupling protein 1 (UCP1). As a proton carrier, UCP1 generates heat by uncoupling the proton transport and ATP production<sup>2</sup>. Upon cold stimulation, thermogenesis in BAT is set in motion by activation of the sympathetic nervous system (SNS), followed by release of norepinephrine (NE). NE binds to the  $\beta 3$  adrenergic receptors and leads to elevation of intracellular cyclic AMP (cAMP). As a consequence, cAMP/PKA-dependent engagement of CREB (cAMP response element-binding protein) stimulates *Ucp1* transcription via direct binding on CREB-response elements (CRE)<sup>2</sup>. In addition to BAT, brown-like adipocytes are also found within white adipose tissue and are therefore named beige or brite (brown-in-white) cells<sup>1,3</sup>. In response to specific stimuli (such as cold), these otherwise quiescent beige cells are remodeled to exhibit multiple brown-like features, including multilocular lipid droplets, densely-packed mitochondria, and augmented UCP1 expression<sup>3-5</sup>.

Animal studies have demonstrated that brown and beige adipocytes possess multiple metabolic benefits beyond its fat-reducing effect, including insulin-sensitization, lipid-lowering, anti-inflammation, and anti-atherosclerosis<sup>6,7</sup>. In humans, the amount of beige/brown fat is inversely correlated with age, insulin resistance index, and cardiometabolic disorders<sup>8</sup>. Moreover, activation of beige/brown adipocytes in humans by either cold acclimation or  $\beta 3$  adrenergic receptor agonist confers protection against a series of metabolic disorders<sup>4,9,10</sup>. These pieces of evidence collectively indicate that induction of brown and beige adipose tissue is a potential therapeutic strategy for management of obesity and its related medical complications<sup>8</sup>.

Interestingly, although they share similar function, beige and classical brown adipocytes are derived from different precursors and activated by overlapping but distinct mechanisms<sup>1</sup>. Therefore, *in vivo* imaging and quantification of brown and beige adipocytes are essential to achieve a better understanding of the molecular control of these adipose tissues. Currently  $^{18}\text{F}$ -fluorodeoxyglucose ([ $^{18}\text{F}$ ]FDG) positron emission tomography (PET) scan combined with computed tomography (CT) remains the gold standard for characterization of thermogenic brown and beige cells in clinical studies<sup>8</sup>. Magnetic resonance imaging (MRI) uses powerful magnetic fields and radio frequency pulses to produce detailed anatomical structures. Compared to CT scan, MRI generates images of organs and soft tissues with a higher resolution. Provided here is a protocol for visualization and quantification of functional brown and beige adiposes in mouse models after acclimation to cold exposure, a common and most reliable way to induce

adipose browning. This method can be applied to characterize the thermogenic adipose depots in small animal models with high precision.

## **PROTOCOL:**

The protocol described below follows the animal care guidelines of The University of Hong Kong. The animals used in the study were 8-week-old C57BL/6J mice.

### **1. Animal surgical procedures and cold challenge**

#### **1.1. Perform interscapular BAT (iBAT) dissection.**

1.1.1. Anesthetize the mice by intraperitoneal injection of ketamine/xylazine. After anesthesia, shave the hair of the mouse from the neck to just below the scapulae.

1.1.2. Place the mice on the heating pad after disinfection and make a 2 cm incision along the dorsal midline of the mice.

1.1.3. Remove the iBAT pads (bilateral). In the sham-operated group, make the same incision but leave the iBAT pads intact.

1.1.4. Close the incision using 7 mm stainless steel wound clips after the bleeding stops.

1.1.5. After surgery, give meloxicam (5 mg/kg) to the mice for 6 days and house them in an intensive care unit (ICU) for 14 days. Remove the clips as soon as the wound is healed (7–10 days).

1.2. Cold challenge of the mice: House the mice at thermoneutrality (30 °C) for 14 days. On day 13, pre-chill the animal cages in cold (6 °C) overnight. On day 14, put the mice at 6 °C in the environmental chamber for 7 days. Place two mice in each cage.

### **2. Micro-PET/MR calibrations and workflow setup**

**NOTE:** Micro-PET/MR imaging is performed using a sequential PET/MR system (see **Table of Materials**). Each mouse is placed on the imaging bed; first scan with the MR for an anatomical reference (scout view) before advancing to the center of the PET field-of-view (FOV) for a static [<sup>18</sup>F]FDG PET acquisition, followed by MR imaging for anatomic reference. An imaging workflow is created in the scanner-operating software (see **Table of Materials**) to enable automated, sequential PET/MR scans prior to the imaging session.

2.1. Create an imaging workflow in the operating software that includes static PET acquisition, MRI acquisitions for attenuation correction, and anatomical reference using T1-weighted 3D imaging and T2-weighted 2D imaging, respectively.

2.2. To acquire PET, set 400–600 keV level discrimination, F-18 study isotope, 1–5 coincidence mode and 20 min scans.

2.3. To acquire T1-weighted MR (for attenuation correction), set Gradient Echo-3D (TE = 4.3 ms, TR = 16 ms, FOV = 90 x 60 mm, number of excitations (NEX) = 3, 28 slices with 0.9 mm thickness, voxel size = 0.375 x 0.375 x 0.9 mm).

2.4. To acquire T2-weighted MR (anatomical reference), set Fast-spin Echo 2D (TE = 71.8 ms, TR = 3000 ms, FOV = 90 x 60 mm, NEX = 5, 32 slices with 0.9 mm thickness, voxel size = 0.265 x 0.268 x 0.9 mm<sup>3</sup>).

2.5. To reconstruct PET, use Tera-Tomo 3D (TT3D) algorithm (8 iterations, 6 subsets) with 1–3 coincidence mode, and with decay, dead-time, random, attenuation, and scatter corrections to create images with an overall of 0.3 mm<sup>3</sup> voxel size.

2.6. Perform a PET Activity Test of the micro-PET/MR scanner one day before the start of imaging study to check the accuracy of PET quantitation.

2.6.1. Prepare a 5 mL syringe filled with [<sup>18</sup>F]FDG as recommended by the manufacturer guidelines (140–220 µCi/5–8 MBq in water or saline).

2.6.2. Record the activity of the syringe using a dose calibrator (see **Table of Materials**) and note the time of measurement.

2.6.3. Select **Interpolated Ellipse ROI** to draw a volume-of-interest (VOI) on the reconstructed image to compare the recovered activity to the value measured as described above. The recovered activity for a well-calibrated scanner is accurate within ±5%.

### 3. Injection of [<sup>18</sup>F]FDG

3.1. Order a clinical dose of [<sup>18</sup>F]FDG (10 mCi/370 MBq) from the supplier for its arrival to the imaging lab approximately 30 min before the first scheduled injection. Make sure to wear appropriate personal protective equipment (PPE), such as a lab coat, gloves, personal finder, and body dosimeters when receiving the package containing radioactive materials. Change gloves regularly to prevent cross contamination of the radioactivity and increase distance from the radioactive source as much as possible.

3.2. Use the forceps to carefully transfer the [<sup>18</sup>F]FDG stock vial behind an L-block table top shield.

3.3. Dispense an aliquot of [<sup>18</sup>F]FDG and dilute with sterilized saline to give a total activity concentration at 200–250 µCi/7–9 MBq) in 100–150 µL.

3.4. Draw the [<sup>18</sup>F]FDG solution into a 1 mL syringe with needle (see **Table of Materials**), measure the radioactivity using a dose calibrator set to F-18, and record the time of measurement.

3.5. Record the weight of the mouse prior to injection. Inject the prepared [<sup>18</sup>F]FDG solution via tail vein. Take note of the injection time and residue of the radioactivity of the syringe to enable decay correction.

3.6. Put the mouse back in the cage and allow [<sup>18</sup>F]FDG uptake for 60 min before PET scans.

3.7. Calculate the injected [<sup>18</sup>F]FDG activity using the following formula<sup>11</sup>:

$$\begin{aligned} \text{Injected activity } (\mu\text{Ci}/\text{MBq}) &= \text{Activity in the syringe before injection} \\ &- \text{activity in the syringe after injection} \end{aligned}$$

#### 4. Micro-PET/MR acquisition

4.1. Turn on the air heater to the mouse bed to allow warm air to pass through it.

4.2. Anesthetize the mouse using 5% isoflurane (1 L/min medical O<sub>2</sub>). Once induced, transfer the mouse to the warm mouse bed and maintain anesthesia at 2%–3 % isoflurane via a nose mask cone. Position the mouse head-prone onto the bite bar and make sure the mouse does not protrude outside of the diameter of the bed. Apply eye lubricant to avoid drying and formation of corneal ulcers.

4.3. Monitor the body temperature and the respiratory rate by a thermal probe and a respiratory pad, respectively. Maintain the body temperature at 36–37 °C, and the respiratory rate at 70–80 breaths per minute (bpm) by adjusting the isoflurane level.

4.4. Perform a scout view to determine the mouse position. Adjust the mouse bed position to include the whole mouse body, and to ensure the center FOV of MR is in the center of mouse body.

4.5. Under the **PET Acquisition** in the study list window, select **Scan Range on Previous Acquisition** to use the scout view position as described above. Click on **Prepare** to move the animal bed from MR to PET. Select **OK** to initiate the PET scan. Record the injection dose and time measured before and after [<sup>18</sup>F]FDG administration in the **Radiopharmaceutical Editor**. Enter the weight of the mouse under the **Subject Information** menu.

4.6. Once the PET scan is completed, select **Prepare** to move to MR and complete all the MR acquisitions in the study list window. Select **OK** to start the MR scans.

4.7. After the whole workflow is completed, briefly evaluate the quality of the acquired MR images using the post-processing software (see **Table of Materials**). Click on the **Home** button to move the mouse bed from MR to the original position.

4.8. Carefully remove the mouse from the scanner and return it to a clean housing cage with a heated pad underneath to allow recovery in warm environment. Supply the mouse with food and water. The system is now ready for the next mouse in queue.

4.9. To reconstruct data, select **PET Acquisition** under the **Raw Scan** menu to load the completed PET scan. Select **T1-weighted MR Acquisition** for material map creation. Reconstruct the data as described above (see step 2.5).

4.10. Follow the local and institute regulations regarding the care and handling of post-PET imaging mouse. Consider all used syringes/needles, gloves, bedding, and fecal matter as radioactive waste that require special handling/disposal in accordance with the local regulations.

## 5. Post-imaging analysis

5.1. Open the **Image Analysis** software (see **Table of Materials**) and click on **Load DICOM Data** to retrieve the corresponding MR and PET images.

5.2. Perform co-registration of MR and PET image by dragging these images to the display window. Click on the **Automatic Registration** function.

5.2.1. Select **Rigid** transformation under the **Registration Setup** drop-down menu. Check **Shift** and **Rotation** under the **Rigid/Affine** menu.

5.2.2. Select **T1-weighted MR acquisition** as the **Reference** and **PET acquisition** as the **Reslice** under the **Global Role Selection** menu.

5.2.3. Inspect the registration in all three dimensions to make sure a perfect alignment between MR and PET images. To adjust it manually, click on **Manual Registration**.

5.3. Use **Interpolated Ellipse ROI** to draw VOI on the tissue of interest, i.e., iBAT and inguinal white adipose tissue (iWAT) using MR image for reference. Use the **Brush Tool** and **Eraser Tool** to define the VOI border; hence, the anatomy of tissues. Make sure there is no overlap uptake by using PET image to avoid spillover from the neighboring organs. Repeat the process slide-by-slide until the whole VOI is delineated. If necessary, edit the VOIs to maintain consistent VOI volumes between each mouse.

5.4. Use **Ellipsoid VOI** to draw a 3 mm<sup>3</sup> VOI on the lung as a reference organ. Avoid any spillover from the neighboring heart and muscle.

5.5. Upon completion, click on **Show ROI Table** to rename each VOI. Record the mean radioactivity with the VOI and tissue volume into a spreadsheet. Archive the VOI drawings and the imaging data to a data storage device.

5.6. Calculate the standardized uptake value (SUV) for all VOIs using the following equation<sup>11</sup>:  
$$\text{SUV}_{\text{mean}} = \text{VOI radioactivity in kBq} / (\text{Decay} - \text{corrected injected dose in kBq} / \text{mouse body weight in kg}), \text{ assuming a tissue density of } 1 \text{ g/mL}.$$

## REPRESENTATIVE RESULTS:

Three groups of mice (n = 3 per group) underwent micro-PET/MR imaging in this study, where they were housed at either thermoneutrality (30 °C) or cold (6 °C) for 7 days. One group of mice (n = 3) had their iBAT removed (iBATx) prior to cold treatment (**Figure 1A**). This method led to an alteration to the white adipose tissue activity in all three mice. In particular, a remarkable increase in [<sup>18</sup>F]FDG uptake was observed in iWAT using micro-PET/MR imaging (**Figure 1B-C**). This co-registered imaging data is demonstrated as maximal intensity projection (MIP), where iWAT was clearly delineated to allow quantification of the [<sup>18</sup>F]FDG uptake. Consistently, the multilocular adipocytes, which are characteristic morphology for beige adipocytes, were more pronounced in iWAT from iBATx mice, compared to the sham operated group (**Figure 1D**).

To verify whether changes on iBAT and iWAT activities upon this prolonged cold induction can be monitored by micro-PET/MR imaging, imaging studies were performed on the mice exposed to 30 °C and 6 °C and the results between groups were compared. PET/MR imaging also demonstrated that mice subjected to 6 °C have markedly elevated [<sup>18</sup>F]FDG uptake on iBAT in sham operated mice (**Figure 2B**), which is consistent with the previous reported literature<sup>11</sup>. Mice with their iBAT removed (iBATx) prior to cold treatment showed the highest [<sup>18</sup>F]FDG uptake in the iWAT among the 30 °C and 6 °C group (**Figure 2A**). PET images were further quantified using an SUV-based approach. In iBAT, cold exposure caused a 7-fold increase in [<sup>18</sup>F]FDG uptake when compared to the 30 °C group. In iWAT, [<sup>18</sup>F]FDG uptake was highest in cold-acclimated iBATx mice than the remaining groups (**Figure 2C**). Removal of iBAT in the cold-induced mice resulted in an 8-fold increase in the uptake compared to the thermoneutrality mice, whereas only a modest increase (2-fold) was observed when iBAT was present in mice.

## FIGURE AND TABLE LEGENDS:

**Figure 1: Micro-PET/MR Imaging of inguinal white adipose tissue (iWAT) in mice.** Interscapular brown adipose tissue was surgically removed (iBATx). After recovery, the mice were housed at 6 °C for 7 days before analysis. **(A)** Flow chart for the surgical and the subsequent procedures. **(B)** Illustration of the position of the mouse and the PET/MR scanner. **(C)** Maximal intensity projection (MIP) of co-registered PET/MR images. White arrows: Location of iWAT. A: Anterior L: Left. **(D)** Hematoxylin and Eosin (HE) staining of iWAT in sham and iBATx mice after cold exposure. Scale bar = 100 µm.



**Figure 2: Representative *in vivo* [<sup>18</sup>F]FDG uptake in brown adipose tissue at the interscapular region (iBAT) and inguinal subcutaneous white adipose tissue (iWAT).** Mice housed at thermoneutrality (30 °C), cold-acclimated (6 °C) and cold-acclimated + iBATx were subjected to [<sup>18</sup>F]FDG PET/MR imaging. **(A)** Sagittal section of PET/MR images showing iBAT in mice. **(B)** Axial section of PET/MR images showing bilateral iWAT. **(C)** Quantitative analysis of [<sup>18</sup>F]FDG uptake in iBAT (left) and iWAT (right). Yellow arrows: Location of iBAT. White arrows: Location of iWAT. n = 3 for each group. Values of SUV<sub>ratio</sub> are presented as mean ± SD.

## DISCUSSION:

In this study, a PET/MR -based imaging and quantification of functional brown and beige adipose tissue in small animal was described. This method uses the non-metabolizable glucose analog [<sup>18</sup>F]FDG as an imaging biomarker so as to identify the adipose tissues with high glucose-demand in a non-invasive manner. MR offers good soft tissue contrast and can better differentiate adipose fat tissues from the neighboring soft tissues and muscle. When combined with PET, this enables imaging and quantifying of the activated adipocytes as a result of high glucose utilization in an accurate manner. The experimental conditions outlined here highlights the feasibility of using [<sup>18</sup>F]FDG PET to study up-regulation of iBAT and iWAT *in vivo*, and is potentially useful for evaluation of the thermogenic impact of new drug candidates. In addition, this protocol can be easily modified into high throughput format by simultaneously imaging multiple mice using a specially designed animal bed, thereby increasing the statistical power and confidence in the imaging data at a reduced cost and time<sup>12,13</sup>.

Currently, [<sup>18</sup>F]FDG PET/CT remains the most common approach to visualize BAT in humans and rodents and standard protocols have been well established<sup>8,11</sup>. In recent years, there are also several studies using [<sup>18</sup>F]FDG PET/MR imaging to assess BAT in humans<sup>14–16</sup>. In contrast, no detailed description on [<sup>18</sup>F]FDG PET/MRI for small animals is available. Described here is a detailed protocol that relies on the use of a combined PET and MR imaging system in mice. This method takes advantage of the higher resolution of MRI, especially on the detection of fat tissues, making them easy to identify and segment compared to the commonly used CT method. Therefore, the current approach enables an improved accuracy of PET quantification compared to the PET/CT method, which is of great value for studies in small animals with more delicate adipose depots. When analyzing the results of tissues of interest at their baseline uptake, MRI becomes an essential tool to accurately draw the VOIs to ensure consistency of their volumes between mice and avoid inclusion of neighboring organs. In addition, accurate image processing such as image registration and VOI delineation are important to allow reliable quantification. The anatomical location of the glucose-responsive BAT is distinct between humans and mouse. While the functional BAT locates at the interscapular region, [<sup>18</sup>F]FDG PET/MR imaging-based analysis mainly identify functional BAT in the supraclavicular region in humans<sup>14–16</sup>.

The fasting or fed status of the mice should also be taken into consideration when performing the [<sup>18</sup>F]FDG uptake experiment. In some studies, the mice are fasted for several hours or even overnight before the uptake experiment since it is supposed that endogenous glucose will compete with [<sup>18</sup>F]FDG. In the protocol, the [<sup>18</sup>F]FDG at fed status was measured and strong uptake signal was still observed in both iBAT and iWAT. This, thus, demonstrates that it is not

necessary to put the mice at a fasted status for robust uptake signals, which is less physiologically relevant. Actually, caution should be taken when examining BAT and beige adipocytes in fasted animals since a previous finding has reported that the hypothalamic neuropeptide Y (NPY)-mediated hunger signal acts on the medullary motor systems to inhibit BAT thermogenesis by reducing the sympathetic innervation<sup>17</sup>. Consistently, in humans, it is suggested that upon high calorigenic diets, the thermogenic adipocytes burn out extra calories so as to maintain energy balance. In contrast, upon nutrient deprivation, counter-regulatory mechanisms are activated to suppress energy waste.

Another consideration for [<sup>18</sup>F]FDG PET imaging involves the routes for radiotracer administration into mice. Intraperitoneal and intravenous techniques are two common ways to inject [<sup>18</sup>F]FDG into mice, and both methods result in a relatively similar biodistribution of [<sup>18</sup>F]FDG in mice 60 min post injection<sup>18</sup>. While the intraperitoneal method is relatively easy to perform and the injection can be done quickly to avoid unwanted stress imposed onto the mice, direct injection accidentally into the bowel is common and is not immediately identified, leading to unreliable PET results<sup>19</sup>. Intravenous method is the preferred method and employed in this study. Successful tail vein injection can be determined when a visible blood flashback is observed prior to infusion, indicating that the needle is properly positioned inside the vein for infusion. One limitation to this technique is the difficulty to notice a visible blood flashback, potentially due to low blood pressure and the presence of dark hair on the tails. This can be overcome by warming the tail with a warm washcloth to increase the blood flow, hence improving the visibility of the vein for needle insertion.

An accurate scanner and a relevant equipment are other important factors for reliable PET image quantification. It is imperative to perform routine quality control examinations on PET and MR components of the scanner. MR quality control involves the signal-to-noise ratio assessment on different T1- and T2-weighted sequences, which should be performed on a weekly basis as recommended by the scanner manufacturer. For PET, accuracy of activity must be determined using a syringe containing a known concentration of radioactivity on a weekly basis or before the start of an important study. This quality control test also allows determination of co-registration of PET and MR images. Calibration must be performed if the recovered activity falls outside the recommended range or mis-registration between PET and MR images is found. In addition, the dose calibrator should be regularly calibrated according to the manufacturer guidelines since this is an important tool for quality control of the scanner as well as radioactivity measurement for PET imaging.

This study shows that the activation of adipose depots in both iBAT and iWAT in mice can be visualized and quantified using [<sup>18</sup>F]FDG PET/MR imaging upon exposure to cold temperature. However, the current study is limited by the fact that [<sup>18</sup>F]FDG uptake in iWAT was relatively low unless in the absence of iBAT. This indicates that compared to the iBAT that is readily activated by cold stimulus, beige adipocytes are relatively reluctant to be mobilized and act more like a backup thermogenic depot of iBAT in mice. More efficient methods to induce the [<sup>18</sup>F]FDG signal in the iWAT and/or other adipose depots in normal mice, such as the use of beige-specific

activators or stronger cold challenge condition, are to be identified, which is beyond the scope of the current study.

#### ACKNOWLEDGMENTS:

We thank the support of Hong Kong Research Grants Council Collaborative Research Fund (CRF C7018-14E) for small animal imaging experiments, and Hong Kong Research Grants Council General Research Fund (GRF 17123419).

#### DISCLOSURES:

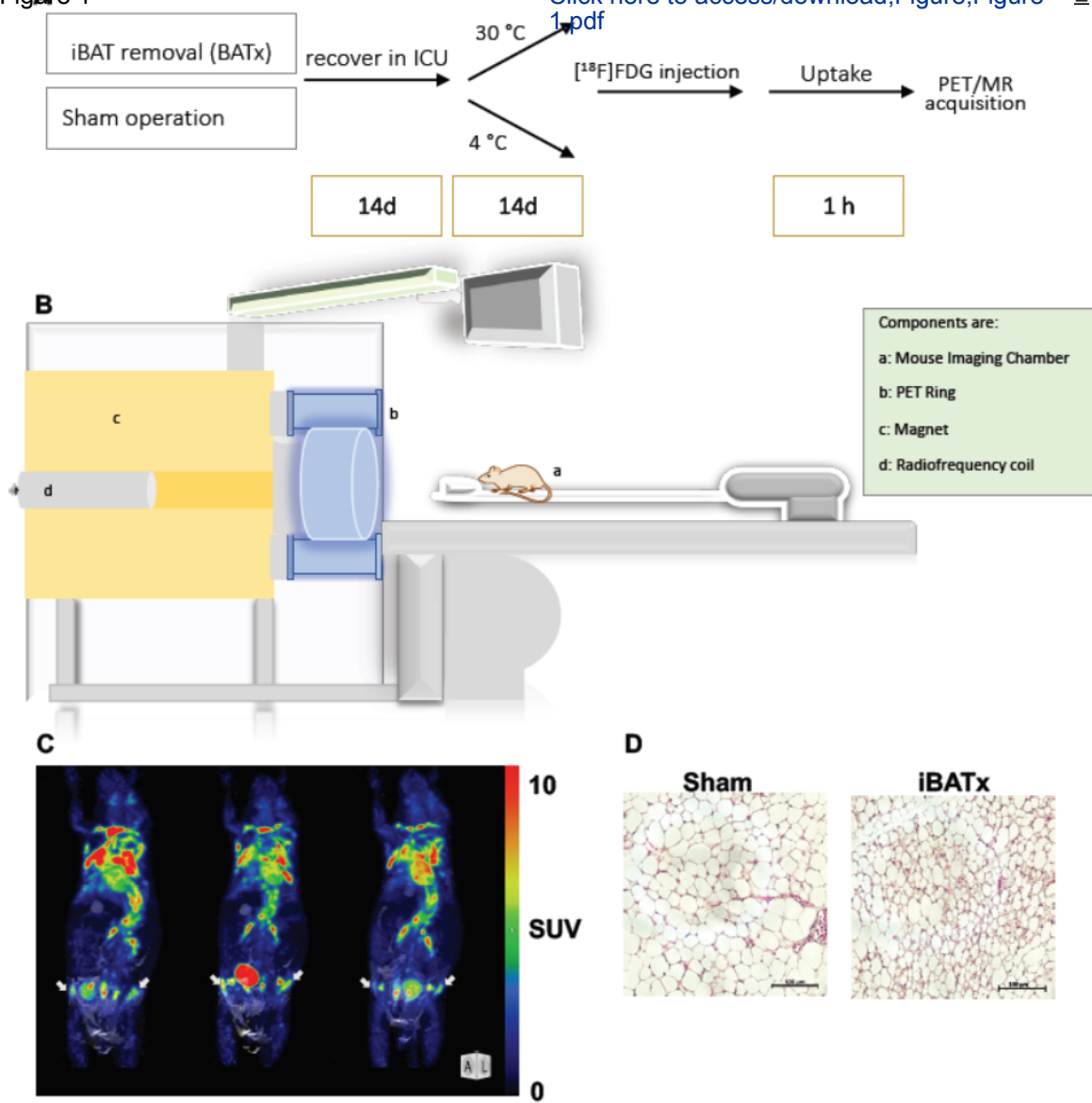
The authors have no conflicts of interest to disclose.

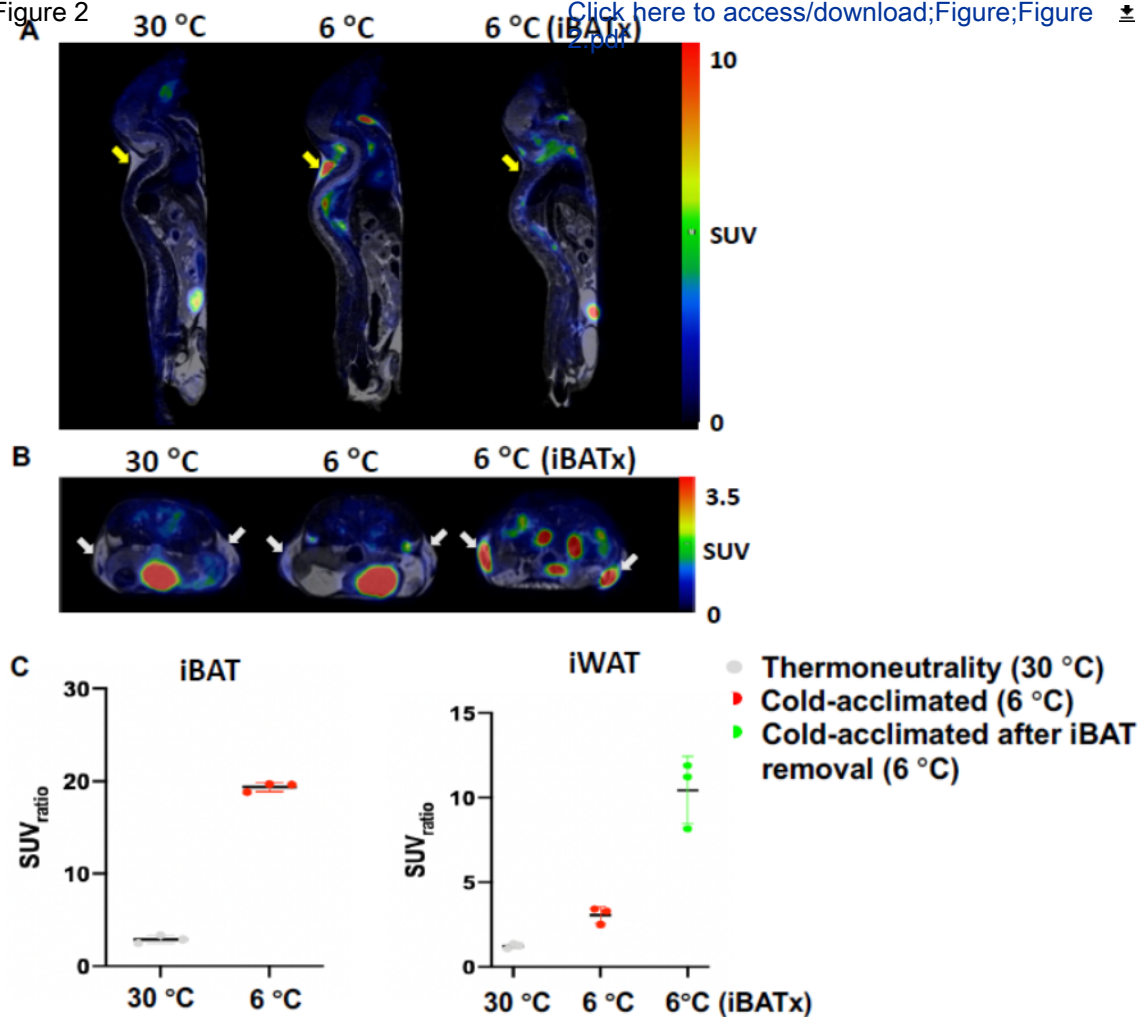
#### REFERENCES:

1. Rosen, E. D., Spiegelman, B. M. What we talk about when we talk about fat. *Cell*. **156** (1–2), 20–44 (2014).
2. Cannon, B., Nedergaard, J. Brown adipose tissue: function and physiological significance. *Physiological Review*. **84** (1), 277–359 (2004).
3. Wu, J. et al. Beige adipocytes are a distinct type of thermogenic fat cell in mouse and human. *Cell*. **150** (2), 366–376 (2012).
4. Cypess, A. M. et al. Activation of human brown adipose tissue by a beta3-adrenergic receptor agonist. *Cell Metabolism*. **21** (1), 33–38 (2015).
5. Ishibashi, J., Seale, P. Beige can be slimming. *Science*. **328** (5982), 1113–1114 (2010).
6. Schulz, T. J. et al. Brown-fat paucity due to impaired BMP signalling induces compensatory browning of white fat. *Nature*. **495** (7441), 379–383, (2013).
7. Cohen, P. et al. Ablation of PRDM16 and beige adipose causes metabolic dysfunction and a subcutaneous to visceral fat switch. *Cell*. **156** (1–2), 304–316 (2014).
8. Cypess, A. M. et al. Identification and importance of brown adipose tissue in adult humans. *New England Journal of Medicine*. **360** (15), 1509–1517 (2009).
9. van der Lans, A. A. et al. Cold acclimation recruits human brown fat and increases nonshivering thermogenesis. *Journal of Clinical Investigation*. **123** (8), 3395–3403 (2013).
10. Hanssen, M. J. et al. Short-term cold acclimation improves insulin sensitivity in patients with type 2 diabetes mellitus. *Nature Medicine*. **21** (8), 863–865 (2015).
11. Wang, X., Minze, L. J., Shi, Z. Z. Functional imaging of brown fat in mice with 18F-FDG micro-PET/CT. *Journal of Visualized Experiments: JoVE*. **69**, e4060 (2012).
12. Greenwood, H. E., Nyitrai, Z., Mocsai, G., Hobor, S., Witney, T. H. High-throughput PET/CT imaging using a multiple-mouse imaging system. *Journal of Nuclear Medicine: Official Publication, Society of Nuclear Medicine*. **61** (2), 292–297 (2020).
13. Carter, L. M., Henry, K. E., Platzman, A., Lewis, J. S. 3D-printable platform for high-throughput small-animal imaging. *Journal of Nuclear Medicine: Official Publication, Society of Nuclear Medicine*. **61** (11), 1691–1692 (2020).
14. Andersson, J. et al. Estimating the cold-induced brown adipose tissue glucose uptake rate measured by (18)F-FDG PET using infrared thermography and water-fat separated MRI. *Scientific Reports*. **9** (1), 12358 (2019).

- 431 15. Lundstrom, E. et al. Brown adipose tissue estimated with the magnetic resonance imaging  
432 fat fraction is associated with glucose metabolism in adolescents. *Pediatric Obesity*. **14** (9),  
433 e12531 (2019).
- 434 16. Lundstrom, E. et al. Magnetic resonance imaging cooling-reheating protocol indicates  
435 decreased fat fraction via lipid consumption in suspected brown adipose tissue. *PLoS One*. **10** (4),  
436 e0126705 (2015).
- 437 17. Nakamura, Y., Yanagawa, Y., Morrison, S. F., Nakamura, K. Medullary reticular neurons  
438 mediate neuropeptide Y-induced metabolic inhibition and mastication. *Cell Metabolism*. **25** (2),  
439 322–334 (2017).
- 440 18. Fueger, B. J. et al. Impact of animal handling on the results of 18F-FDG PET studies in mice.  
441 *Journal of Nuclear Medicine: Official Publication, Society of Nuclear Medicine*. **47** (6), 999–1006  
442 (2006).
- 443 19. Vines, D. C., Green, D. E., Kudo, G., Keller, H. Evaluation of mouse tail-vein injections both  
444 qualitatively and quantitatively on small-animal PET tail scans. *Journal of Nuclear Medicine*  
445 *Technology*. **39** (4), 264–270 (2011).
- 446

**Figure 1** [Click here to access/download;Figure;Figure 1.pdf](#)





Name of Material/Equipment	Company	Catalog Number	Comments/Description
0.9% sterile saline	BBraun		0.9% sodium chloride intravenous infusion, 500 mL
5 mL syringe	Terumo	SS05L	5 mL syringe Luer Lock
Dose Calibrator	Biodex		Atomlab 500
Eye lubricant	Alcon Duratears		Sterile ocular lubricant ointment, 3.5 g
Insulin syringe	Terumo	10ME2913	1 mL insulin syringe with needle
InterView Fusion software	Mediso	Version 3.03	Post-processing and image analysis software
Isoflurane	Chanelle Pharma		Iso-Vet, inhalation anesthetic, 250 mL
Ketamine	Alfasan International B.V.	HK-37715	Ketamine 10% injection solution, 10 mL
Medical oxygen	Linde HKO	101-HR	compressed gas, 99.5% purity
Metacam	Boehringer Ingelheim		5 mg/mL Meloxicam solution for injection for dogs and cats, 10 mL
nanoScan PET/MR Scanner	Mediso		3 Tesla MR
Nucline nanoScan software	Mediso	Version 3.0	Scanner operating software
Wound clips	Reflex 7	203-100	7mm Stainless steel wound clips, 20 clips
Xylazine	Alfasan International B.V.	HK-56179	Xylazine 2% injection solution, 30 mL

## Point-by-point responses

(Manuscript ID: JoVE62460 by Liu et al)

We would like to express our thanks to the reviewers' comments. We have revised our manuscript by including additional data and clarifications. Our point-by-point responses to all the comments by the editor and the reviewers are as follows.

### Responses to Editor

1. *Please take this opportunity to thoroughly proofread the manuscript to ensure that there are no spelling or grammar issues.*

**Reply:** We have had the manuscript proofread by a native speaker so that there shall be minimal spelling or grammar issues in the current version.

2. *Please revise the following lines to avoid previously published work: 128-130, 146, 148-150, 189-190, 233-234, 277-280.*

**Reply:** These lines have been revised.

3. *Please provide an institutional email address for each author.*

**Reply:** Institutional email address for Dr. Liu has now been provided.

4. *Please provide at least 6 keywords or phrases.*

**Reply:** 6 keywords have now been provided.

5. *JoVE cannot publish manuscripts containing commercial language. This includes trademark symbols (™), registered symbols (®), and company names before an instrument or reagent. Please remove all commercial language from your manuscript and use generic terms instead. All commercial products should be sufficiently referenced in the Table of Materials.*

**Reply:** Commercial language within the manuscript has now been replaced by generic terms.

6. *Please include an ethics statement before your numbered protocol steps, indicating that the protocol follows the animal care guidelines of your institution.*

**Reply:** The said statement has been added before the protocol number.

7. *Please adjust the numbering of the Protocol to follow the JoVE Instructions for Authors. For example, 1 should be followed by 1.1 and then 1.1.1 and 1.1.2 if necessary. Please refrain from using bullets or dashes.*

**Reply:** The numbering of the Protocol has now been adjusted to conform to the JoVE Instructions.

8. *Line 79-86: The Protocol should be made up almost entirely of discrete steps without large paragraphs of text between sections. Please simplify the Protocol so that individual steps contain only 2-3 actions per step and a maximum of 4 sentences per step.*



**Reply:** We now split the protocol to numbered steps with each step contains less than 4 sentences.

9. Line 84: *Please specify the dose of meloxicam used.*

**Reply:** The dose of meloxicam has been provided in the manuscript.

10. Line 93-98: *Please ensure that all the steps are numbered. We cannot have non-numbered paragraphs/steps/headings/subheadings.*

**Reply:** OK.

11. Line 139: *Please use standard abbreviations for time units preceded by a numeral. Examples: 5 h, 10 min, 100 s, 8 days, 10 weeks*

**Reply:** We now checked throughout the manuscript to ensure standard abbreviations for time units are used.

12. *Please include a one-line space between each protocol step and highlight up to 3 pages of the Protocol (including headings and spacing) that identifies the essential steps of the protocol for the video, i.e., the steps that should be visualized to tell the most cohesive story of the Protocol. Remember that non-highlighted Protocol steps will remain in the manuscript, and therefore will still be available to the reader.*

**Reply:** Essential steps for the video have been highlighted.

13. *Please title case and italicize journal titles and book titles. Do not use any abbreviations. Article titles should start with a capital letter and end with a period and should appear exactly as they were published in the original work, without any abbreviations or truncations. Please do not use the &-sign or the word “and” when listing authors.*

**Reply:** The format of the references has been checked.

14. *Please remove the titles and Figure Legends from the uploaded figures. The information provided in the Figure Legends after the Representative Results is sufficient.*

**Reply:** The titles and legends were removed from the figures.

15. Figure 1B: *Please include scale bars in all the images of the panel. Please include the details of magnification in the Figure Legends.*

**Reply:** Scale bars are added in the images and the length of the scale bar is indicated in the legends.

## Responses to Reviewer #1

**Reviewers' Comments:** The manuscript faces an interesting topic, though not commonly found in literature. Indeed, this argument can be deeply studied with FDG PET/CT, also in human settings.

Major Concerns:

1. *It might be interesting arguing about a comparison between what you obtained in your study and what emerged from human studies, also using FDG PET/MRI. See "Andersson J, Lundström E, Engström M, Lubberink M, Ahlström H, Kullberg J. Estimating the cold-induced brown adipose tissue glucose uptake rate measured by 18F-FDG PET using infrared thermography and water-fat separated MRI. Sci Rep. 2019 Aug 26;9(1):12358." and "Lundström E, Ljungberg J, Andersson J, Manell H, Strand R, Forslund A, Bergsten P, Weghuber D, Mörwald K, Zsoldos F, Widhalm K, Meissnitzer M, Ahlström H, Kullberg J. Brown adipose tissue estimated with the magnetic resonance imaging fat fraction is associated with glucose metabolism in adolescents. Pediatr Obes. 2019 Sep;14(9):e12531." or "Lundström E, Strand R, Johansson L, Bergsten P, Ahlström H, Kullberg J. Magnetic resonance imaging cooling-reheating protocol indicates decreased fat fraction via lipid consumption in suspected brown adipose tissue. PLoS One. 2015 Apr 30;10(4):e0126705." for more details.*

**Reply:** Thanks the reviewer for the constructive comment. In the revised discussion section, a paragraph discussing and comparing the findings between ours and those in human studies has been added. Briefly, 18-FGF/MRI based studies in humans mainly reveal functional BAT in the supraclavicular region.

2. *What were the limits of your study?*

**Reply:** The current study is mainly limited by the fact that our current protocol of cold challenge only causes a weak induction of glucose uptake in inguinal subcutaneous adipose tissue (iWAT). Therefore study has to be performed in mice with the removal of the interscapular BAT, in which glucose uptake and biogenesis of beige adipocytes were prominent. More efficient method to induce beige adipocytes in the iWAT and/or other adipose depots in normal mice are to be identified, which is beyond the scope of the current study. This limitation has now been added in the last paragraph of the discussion section.

Minor Concerns:

None.

## Responses to reviewer #2

*The reviewer's comment:* The authors reported on a protocol for quantitative brown fat activation detection with 18F-FDG PET imaging by SUV calculation and simultaneous MR imaging for better anatomic delineation of iBAT and inguinal WAT in mice. 9 mice were distributed into 3 groups with 3 mice each, where one group was kept at thermoneutrality, one group at 6°C with removed iBAT, and one group at 6°C that only had a sham surgery. Higher SUV was found for the cold acclimated cohorts, especially for the cohort with removed iBAT.

The surgery procedure and image analysis steps including post-processing steps were described. The text reads well, but I have some doubts whether really the up-to-date technique was described and whether the up-to-date literature was considered in both Introduction, study design and Discussion part.

Major Concerns:

*1) It would be helpful to have a visualization in form of a flow chart the preparation steps you are describing, such as the mouse preparation procedure. Delineation of the anatomy on photographic images or sketches would complement the explanation of how surgery was done step by step.*

**Reply:** Thank the reviewer for this constructive suggestion. A flow chart describing the preparation steps is provided as Figure 1A. For surgery procedures, video will be taken in which the anatomy of the mice will be clearly shown.

*2) As the mouse positioning was described in the text, a schematic drawing of the PET/MR scanner including the mouse positioning would be desirable.*

**Reply:** A schematic drawing including the PET/MR scanner and the mouse positioning is proved as Figure 1B. The detailed positioning of the mouse will also be demonstrated in the video.

*3) Since MR was available - why not adding some quantitative scans such as chemical-shift-separated water-fat imaging for quantification of changes in fat fraction, or T1 mapping?*

*For a summary of potential MR parameters to look at, consider:*

*\* DOI: 10.3389/fendo.2020.00421*

**Reply:** We thank the reviewer for suggesting the addition of the more advance MR imaging techniques for BAT quantification besides the FDG-PET scans proposed in this study. We feel that however inclusion of MR quantification scans is beyond the aim and scope of the current study, which is to investigate the glucose utilization on both BAT and WAT in vivo using FDG-PET. In addition, MR scans performed in this study serve as an anatomic reference to PET scans, where the excellent soft tissue contrast is sufficient to allow visualization and delineation of BAT and WAT,

which is not possible to achieve as reported previously using CT scans. Advance MR imaging techniques proposed by the reviewer certainly warrant thorough investigation and optimization on the preclinical scanner, and these kind of studies are currently underway in our laboratory which we hope to report the findings in due course.

4) *In my opinion it is not feasible to do statistically significant tests at this low number of animals per cohort. Could you then also specify which test you used for calculating the p-values? This was missing in both the text and the figure caption. I think it would be enough showing the results for the mice measured, and leaving out the statistical component as this was not the intention of the paper anyhow, if I understood correctly.*

**Reply:** We agree with the reviewer that the statistical tests were not feasible due to the low number of animals used. Thus we have now deleted the statistical component in Figure 2, as suggested by the reviewer.

Abstract:

5) *Line 24-25: To my knowledge BAT is still in an early research stage and how to use it as a therapeutic target is still very unknown. Dangerous hyperthermia conditions have resulted from early tests.*

**Reply:** Yes the reviewer is correct that BAT is potential but not yet new therapeutic targets for diseases. This statement is toned down.

Introduction:

6) *Line 60: Here you say correctly, that it is a potential target for therapy of obesity, but only potential! Please adapt in the abstract.*

**Reply:** Indeed claiming BAT as a potential target is more appropriate. We have rectified the overstatement in the abstract.

Discussion

7) *Line 268-280: In contrary as stated by the authors, fasting status is important to control when examining BAT activation, as shown for instance in:*

*Postprandial activation of BAT: \* DOI: 10.1016/j.cell.2018.10.016*

**Reply:** We compared the FDG uptake in both fasting and fed mice and our results showed that glucose uptake in BAT was minimized after the mice were fasted overnight. This study (DOI: 10.1016/j.cell.2018.10.016) demonstrated that secretin, which is elevated after meal, mediates prandial thermogenesis in BAT, which consequentially induces satiation. Therefore this study is consistent with our notion that BAT is more activated in fed state of the mice.

8) Please read and consider following publications on PET/MR scanning of BAT in humans:

<https://doi.org/10.1002/oby.22560>

doi: 10.1002/mrm.26589

**Reply:** We do notice that there are several PET/MRI studies for assessment of BAT in humans.

We have now discussed and compared the findings in humans and in mice by us in the discussion section. Briefly, 18-FGF/MRI based studies in humans mainly reveal functional BAT in the supraclavicular region.

9) Line 314-315: How would the authors suggest to suppress iBAT activity and how to selectively activate beige adipose tissue? Do the authors have any reference literature? And more importantly: WHY would that be of interest?

**Reply:** There are studies indicating that impairment on classical BAT induces beige cell biogenesis in iWAT, as described in the studies: (1) Brown Fat Paucity Due to Impaired BMP Signaling Induces Compensatory Browning of White Fat. *Nature*. 2013 Mar 21; 495(7441): 379–383. (2) Prdm16 is required for the maintenance of brown adipocyte identity and function in adult mice. *Cell Metab*. 2014 Apr 1; 19(4): 593–604. Lin et al. reported that administration of GC-1, the thyroid hormone receptor beta (TR  $\beta$ ) agonist, induces multilocular beige adipocytes in iWAT (Pharmacological Activation Of Thyroid Hormone Receptors Elicits A Functional Conversion Of White To Brown Fat. *Cell Rep*. 2015 Nov 24; 13(8): 1528–1537.) Several flavonoids have also been demonstrated as inducers of beige adipocytes, which is reviewed by Zhang et al. (Flavonoids as inducers of white adipose tissue browning and thermogenesis: signalling pathways and molecular triggers. *Nutrition & Metabolism*. 2019; 16: 6022).

Therefore, although in the current study, only a weak glucose uptake was induced in iWAT, the protocol described for measurement of glucose uptake and functionality in iWAT would be of interest for other researchers for evaluation of pharmacological reagents, or characterization of specific animal models.

10) Could you please indicate what kind of mice were used? special genetic sort?

**Reply:** We are using 8-week-old C57BL/6J mice. This information is now provided at the beginning of the protocol.

*Minor Concerns:*

Line 140: Please add reference to given formula.

**Reply:** A reference is added.

*Line 155: ... body temperature and the respiratory ...*

**Reply:** The missing word “and” has been added.

*Line 154-155: please check wording/grammar of this sentence*

**Reply:** This sentence is rectified as “Adjust the mouse bed position to include the whole mouse body, and to ensure the center FOV of MR is located in the center of mouse body.”.

*Line 188: using the MR image for reference*

**Reply:** The sentence has been rectified. Thank you.

*Line 198-200: please add reference to equation*

**Reply:** A reference is added.

*Line 210: ..., that are ...*

**Reply:** This typo has been corrected.

*Line 215: are you here referring to in this case sham operated or iBATx?*

**Reply:** Here we are referring to sham operated mice. We now further clarified this point in the description.